# Advancing Micro to Nanoplastic Quantification in Fine Particles using Pyrolysis-Gas Chromatography-Mass Spectrometry

Jianchu Ma[1,2], Shizhen Zhao[*1], Kun He[1,2], Lele Tian[1,2], Linbo Yu[1], Guangcai Zhong[1], Jun Li[1], Qisheng Zhou[3], Duohong Chen[3], Kewei Chen[4,5], Gan Zhang[1]

[1] State Key Laboratory of Organic Geochemistry and Guangdong Key Laboratory of Environmental Resources Utilization and Protection, Guangzhou Institute of Geochemistry, Chinese Academy of Sciences, Guangzhou 510640, China

[2] University of Chinese Academy of Sciences, Beijing 100049, China

[3] Environmental Key Laboratory of Regional Air Quality Monitoring, Ministry of Ecology and Environment, Guangdong Ecological Environment Monitoring Center, Guangzhou 510308, China

[4] Frontier Laboratories Ltd., 4-16-20 Saikon, Koriyama, Fukushima 9638862, Japan

[5] Evertech Instrument Technology Ltd., Guangzhou 510320, China

*Corresponding author:

Shizhen Zhao

Email: zhaoshizhen@gig.ac.cn

# Abstract

Microplastics and nanoplastics (MNPs) are globally concerning for human health because of their ubiquity, persistence, and potential toxicity, especially when bound to atmospheric fine particles ($PM_{2.5}$). Traditional quantification using pyrolysis-gas chromatography-mass spectrometry (Py-GC/MS) often struggles with accuracy because of false positives from similar polymers and organic compounds. In this study, we developed a reliable analytical strategy to enhance the precision of Py-GC/MS for $PM_{2.5}$-bound MNPs. We introduced a chromatographic reconstruction procedure that minimized quantitative interference among polymers, achieving high accuracy (>89%) for polyvinyl chloride, polyethylene terephthalate, and polystyrene, which are commonly overestimated due to overlapping pyrolysis products. Furthermore, we developed an efficient $HNO_3$ digestion method that removed organic matter within two hours under high-pressure oxidation conditions with a recovery rate of 60%–98% for eight target polymers, marking a substantial improvement over previous methods. Applying these new methods, we examined the occurrence and composition of MNPs in $PM_{2.5}$ from urban Guangzhou, finding concentrations from 99.7 to 982.8 ng/m$^3$, with polyethylene, polyethylene terephthalate, and polyvinyl chloride making up more than 90% of the total detected polymers. This improved Py-GC/MS technique offers a robust solution for accurately determining MNPs in fine particles, facilitating future research on their environmental behavior and risk assessment.



# Keywords

Microplastics, nanoplastics, fine particles, urban air, pyrolysis-gas chromatography mass spectrometry, quantitative interference, nitric acid digestion;


# Synopsis

The study presented an innovative strategy to reduce quantitative interference from

polymers and organic matter in characterizing urban $PM_{2.5}$-bound micro to nanoplastics with pyrolysis-gas chromatography-mass spectrometry.

## TOC

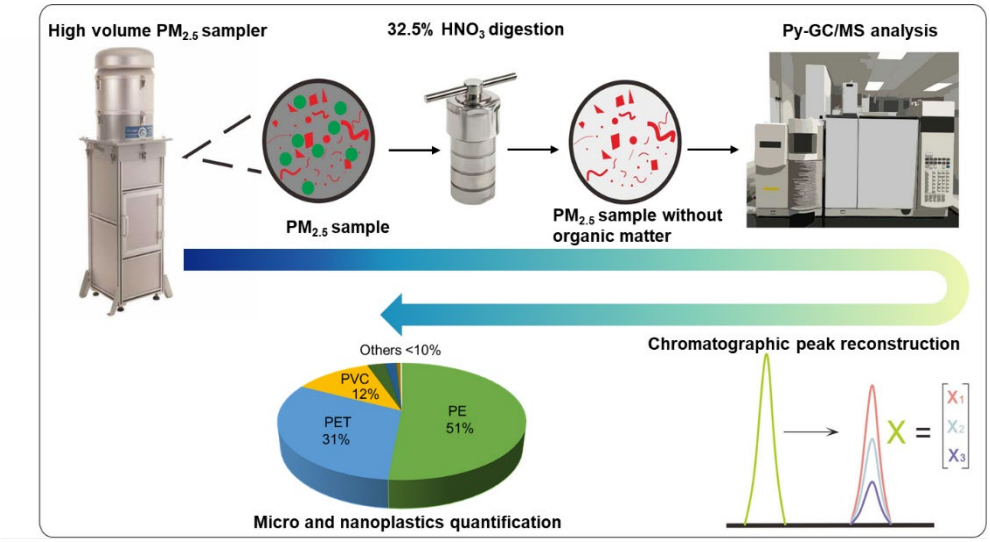

# 1. Introduction

As emerging environmental pollutants, microplastics (1–5 μm) and nanoplastics (<1 μm) have garnered significant attention due to their ubiquitous presence in the environment and their associated health risks.[1,2] The atmosphere serves as a major source and sink for micro and nanoplastics (MNPs).[3,4] Atmospheric MNPs have been reported worldwide, even in remote regions such as the Arctic[5] and the Tibetan Plateau.[6] Due to higher human activities, the levels of MNPs in an urban atmosphere exceed those in remote regions.[7–11] MNP exposure can cause adverse effects on biota,[12–14] including damage to the neurological and hepatic function in mice[15] and a decrease in the hatching rate of zebrafish.[16] In addition, MNP exposure in humans may significantly increase the risk of cardiovascular disease and stroke.[17] Inhalation is considered the primary route of human exposure to MNPs.[12,14,18] Atmospheric suspended particles with an aerodynamic diameter ≤2.5 μm ($PM_{2.5}$) can enter the human body via the respiratory tract.[19] Therefore, MNPs of $PM_{2.5}$ pose a greater threat to human health. However, research is still limited, with only four articles reporting MNP pollution levels in $PM_{2.5}$ of maximum concentrations up to 25 $\mu g/m^3$.[20–23] These findings underscore the urgent need for a comprehensive characterization of the occurrence and composition of $PM_{2.5}$-bound MNPs to fully assess their human and other biota health risks.

Optical characterization methods, such as micro-Fourier transform infrared spectroscopy (μ-FT-IR) and Raman spectroscopy, are widely used to identify and quantify atmospheric MNPs.[7–11] However, these optical methods cannot provide the mass concentration of MNPs and their results can be affected by subjective judgment.[24,25] Additionally, optical methods face challenges in measuring MNPs with particle sizes <5 μm.[26] Plastics are more likely to degrade into nanoplastics in the atmosphere due to weathering and photooxidation.[27] Consequently, measurement results based on optical methods will undoubtedly overlook nanoplastics. In contrast, the identification and quantification of MNPs through pyrolysis-gas chromatography mass spectrometry (Py-GC/MS) rely on their characteristic pyrolysis products.[28,29] This

technique is not limited by the complex physical properties, such as size, shape, and color, of MNPs and therefore provides more objective measurement results.[30,31] Hence, it is considered a promising technique for MNP analysis.

However, the determination of MNPs by Py-GC/MS faces two primary challenges.[32] One significant aspect arises from internal interference among MNPs. Different polymers may produce the same pyrolysis products, resulting in false positives when these products (considered nonspecific) are chosen for polymer identification and quantification.[33,34] For instance, the characteristic products for quantifying polyvinyl chloride (PVC), such as benzene and naphthalene,[35] can also be generated during the pyrolysis of polyethylene terephthalate (PET) and polystyrene (PS),[36,37] leading to an overestimation of PVC. Another well-known interference results from organic matter because it can generate characteristic pyrolysis products of MNPs.[34,38,39] For example, natural fats and waxes release straight-chain alkanes during pyrolysis,[40] while lignin releases aromatic compounds such as benzene and naphthalene.[41,42] Atmospheric $PM_{2.5}$ contains various organic components that interfere with MNP determination, including volatile compounds, such as indene and naphthalene,[37,43] and recalcitrant organic matter, such as pollen and humic acid.[36,44–46] Therefore, sample pretreatment is needed to remove organic matter. However, current research on $PM_{2.5}$-bound MNPs lacks an understanding or description of effective pretreatment steps,[20–23] which may increase the uncertainty of MNP results.

In this study, we developed a reliable analytical strategy for the identification and quantification of $PM_{2.5}$-bound MNPs using Py-GC/MS; the most commonly used plastics, polyethylene (PE), polypropylene (PP), PVC, PET, PS, polycarbonate (PC), polymethylmethacrylate (PMMA), and acrylonitrile butadiene styrene copolymers (ABS) were target polymers. To achieve this, we proposed a quantification and pretreatment procedure to eliminate interference from co-producing polymers and organic matter. Subsequently, we employed these procedures to examine the presence and composition of MNPs in urban $PM_{2.5}$ samples collected from Guangzhou (southern

China). Thus, we propose a novel methodology for quantifying MNPs in atmospheric $PM_{2.5}$, providing a foundation for further investigation into their pollution levels and health risks.

# 2. Materials and Methods

## 2.1. MNP Standards

To minimize weighting uncertainty and attain low calibration concentrations consistent with concentrations in environmental samples, six polymer solution standards and two polymer solid standards were prepared according to previous research.[47] In brief, specific polymers, such as PS, ABS, PVC, PC, and PMMA, were dissolved in a mixed solution of dichloromethane and tetrahydrofuran (TFA) with a volume ratio of 1:1. Deuterated polystyrene-d8 (d-PS) was dissolved in ethyl acetate, PET and PA6 were solubilized in hexafluoroisopropanol, and PE and PP were diluted with silica and homogenized by a cryo-mill (IQ-mill-2070, Frontier Laboratories Ltd., Japan). The concentrations of each polymer standard are shown in Table S1.

## 2.2 Py-GC/MS Analysis

The Py-GC/MS analysis was conducted using an EGA/PY-3030D pyrolizer (Frontier, Japan) fitted with an Agilent 7890A GC instrument (Agilent, Santa Clara, CA, USA) and connected to an Agilent 5975C quadrupole MS detector (Agilent, Santa Clara, CA, USA), which was operated in EI mode. A DB-5MS column (30 m × 0.25 mm × 0.18 μm; Agilent, Santa Clara, CA, USA) was used for GC separation. The double shot mode was used for the sample pyrolysis. A thermal desorption procedure was employed to minimize interference from coexisting volatile substances before pyrolysis.[43,48] Additional details are available in Text S1 and Table S3.

The selection of characteristic pyrolysis products for polymer identification and quantification was based on previous studies,[5,37,49] as shown in Table S2. Specifically, $C_{20}$ α-alkane was selected as the quantitative product for PE due to a lower likelihood

of generation from organic matter.[28] For PET, benzene was chosen as the quantitative product due to its specific pyrolysis product, benzoic acid, that exhibits poor chromatographic capability.[50,51] In the case of PVC, indene was selected as the quantitative product, given that the yields of its specific pyrolysis product, chlorobenzene, are limited.[52,53] The total ion chromatogram and the extracted ion chromatograms for the selected quantitative products of the target polymers in the mixed polymer standard are presented in Figure 1.

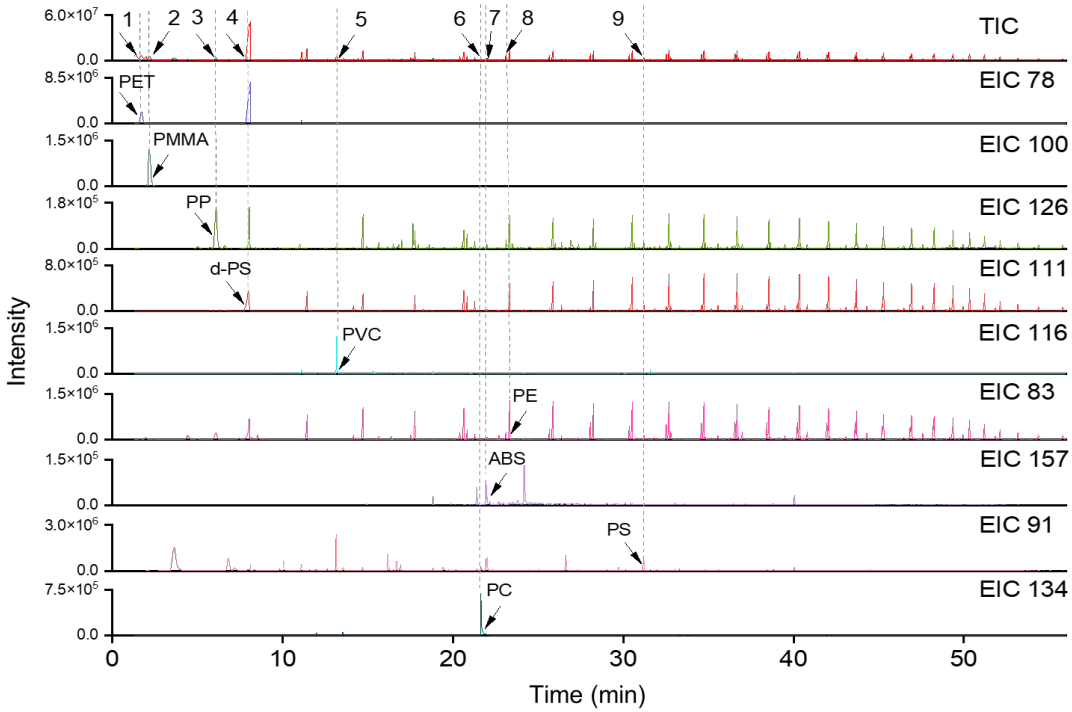


Figure 1. Total ion chromatogram of the mixed polymer standard and extracted ion chromatograms of selected indicator ions for PET (m/z 78, benzene, peak 1), PMMA (m/z 100, methyl methacrylate, peak 2), PP (m/z 126, 2,4-dimethyl-1-heptene, peak 3), d-PS (m/z 111, styrene-d7, peak 4), PVC (m/z 116, indene, peak 5), PC (m/z 134, 4-(1-methyl ethyl)phenol, peak 6), ABS (m/z 78, 4-phenyl-4-pentenenitrile, peak 7), PE (m/z 78, C20 α-alkane, peak 8), and PS (m/z 78, styrene trimer, peak 9).

## 2.3 Identification of Internal Interference

We investigated the specificity of selected quantitative products from each polymer, as well as the potential internal interference induced by the selection of nonspecific products. Equal masses (10.0 μg) of each single polymer standard were analyzed under

identical instrumental conditions. The ions corresponding to the selected quantitative products (Table S2) for all polymers were extracted from the chromatogram of each single polymer standard. If a characteristic product used for quantifying a specific polymer was detected in that polymer's standard and in standards of other polymers of equal mass, and the response in those other polymer standards was within two orders of magnitude of the response in the specific polymer standard, then we considered it a nonspecific product. The polymers responsible for generating the nonspecific product were then identified as mutual interference polymers.

### 2.4 Quantification of MNPs

MNPs typically exist in the environment as mixtures, which can lead to co-pyrolysis effects during pyrolysis, thereby resulting in changes in the response of its products.[54–56] To better simulate the presence of MNPs in environmental samples, mixed polymer standards were prepared by combining eight individual polymer standards. These mixed standards were then used to construct calibration curves, with the aim of reducing uncertainties from co-pyrolysis effects. Additionally, d-PS was added to the mixed polymer standards and samples to act as an internal standard. The calibration curves were constructed using the mass of each polymer in the mixed polymer standards and the response factor for their respective quantification ions (Table S2). The amount of polymer in the samples was calculated using its corresponding response factor and calibration curve.

For polymers with nonspecific quantitative products, we developed a distinct methodology (mathematical algorithm) for constructing their calibration curve and quantifying their presence in samples, which was based on previous studies.[37,57] The algorithm reconstructs the chromatographic peaks of these nonspecific products into a linear combination of contributions from polymers responsible for their generation. The main principle and workflow of the chromatographic peak reconstruction and quantification are illustrated in Figure 2.

In the first step, multiple mass gradients of mixed polymer standards were analyzed by Py-GC/MS. The response factors (i.e., the ratio of a quantitative ion's peak area for a particular polymer to the internal standard) of quantitative ions for the mutual interference polymers in mixed standards were calculated and combined into a matrix (box 1 in Figure 2). In the second step, various mass gradients of single standards were analyzed and their response factors determined. Assuming a consistent generation rate of each polymer pyrolysis product, it was possible to formulate a linear equation that expresses the response factor ratio of the polymer's quantitative products as a result of its resulting nonspecific products based on polymer single standards (box 2 in Figure 2). These equations suggest a quantitative relationship between the contributions of mutual interference polymers to each nonspecific product. Therefore, a source contribution matrix of nonspecific products can be derived from these equations.

In the third step, nonspecific products in the MNP mixture were hypothesized to primarily result from the linear combination of contributions from the mutual interference polymers. By resolving the response factors matrix from mixed standards and the source contributions matrix of nonspecific products from single standards (box 3 in Figure 2), a reconstructed chromatographic peak matrix was obtained (box 4 in Figure 2). This matrix represents the actual response factor for mutual interference of the polymers. The estimated solution does not allow negative values for the unknowns (i.e., no negative contribution from polymers). The solving process was achieved by using a least-squares approximation method (R, v4.12).

In the fourth step, the reconstruction process was applied to each mass gradient of the mixed polymer standard. The model fit was evaluated by comparing the reconstructed response factors and their initially determined values (box 5 in Figure 2). Then, the obtained actual response factor for mutual interference of the polymers and their corresponding mass was used to construct the calibration curve (box 6 in Figure 2). Finally, the reconstruction process and the calibration curve were used to quantify the amount of polymers that are frequently overestimated in the environmental samples due

to the overlapping of pyrolysis products (box 7 in Figure 2).

To test the performance of the quantification procedure for MNP mixtures, a set of different masses of commercially mixed MNP standard (Frontier, Japan) was analyzed and quantified using our proposed process. The quantification accuracy was calculated using Eq. 1:

$$Accuracy = \frac{m_C}{m_T} \times 100\% \quad \text{(Eq. 1)}$$

where $m_C$ (μg) is the calculated mass of the MNP mixed standard determined by our quantification procedure, and $m_T$ (μg) is the expected mass of the MNP mixed standard.

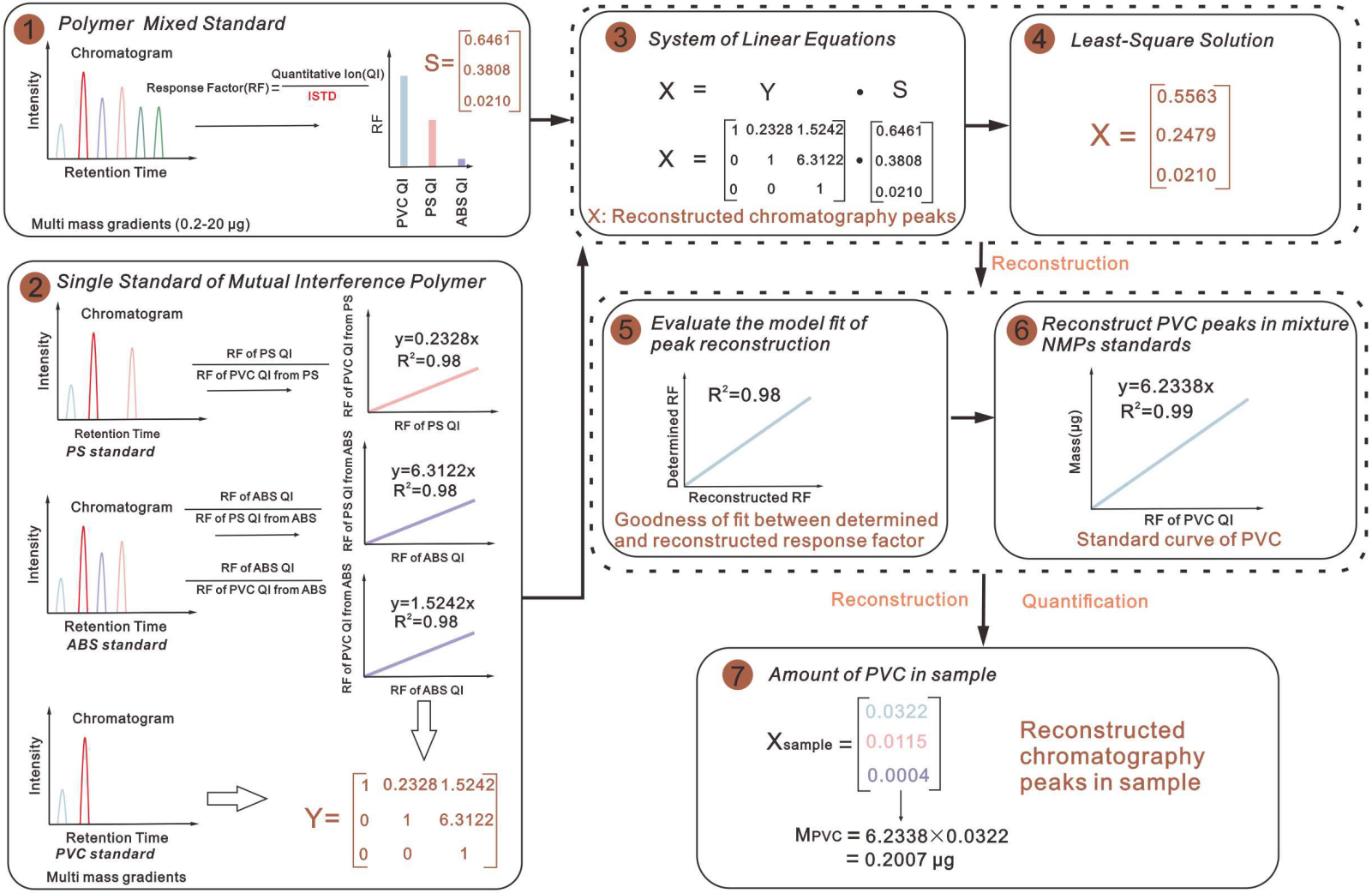
1 Polymer Mixed Standard
Chromatogram
Intensity
Retention Time
Response Factor(RF) = Quantitative Ion(QI) / ISTD
S= 0.6461 0.3808 0.0210
RF
PVC QI
PS QI
ABS QI
Multi mass gradients (0.2-20 μg)
2 Single Standard of Mutual Interference Polymer
Chromatogram
Intensity
Retention Time
PS standard
RF of PS QI
RF of PVC QI from PS
RF of PVC QI from PS
y=0.2328x
R²=0.98
RF of PS QI
Chromatogram
Intensity
Retention Time
ABS standard
RF of ABS QI
RF of PS QI from ABS
RF of PS QI from ABS
y=6.3122x
R²=0.98
RF of ABS QI
RF of ABS QI
RF of PVC QI from ABS
RF of PVC QI from ABS
y=1.5242x
R²=0.98
RF of ABS QI
Chromatogram
Intensity
Retention Time
PVC standard
Multi mass gradients
Y= 1 0.2328 1.5242 / 0 1 6.3122 / 0 0 1
3 System of Linear Equations
X = Y • S
X = 1 0.2328 1.5242 / 0 1 6.3122 / 0 0 1 • 0.6461 0.3808 0.0210
X: Reconstructed chromatography peaks
4 Least-Square Solution
X = 0.5563 0.2479 0.0210
Reconstruction
5 Evaluate the model fit of peak reconstruction
Determined RF
R²=0.98
Reconstructed RF
Goodness of fit between determined and reconstructed response factor
6 Reconstruct PVC peaks in mixture NMPs standards
Mass(μg)
y=6.2338x
R²=0.99
RF of PVC QI
Standard curve of PVC
Reconstruction
Quantification
7 Amount of PVC in sample
Xsample = 0.0322 0.0115 0.0004
Reconstructed chromatography peaks in sample
MPVC = 6.2338×0.0322
= 0.2007 μg

Figure 2. Principle and workflow of the chromatographic peak reconstruction and quantification procedure proposed in this study. The example shown is for peak reconstructions of PVC and PS. The response factors of indene (PVC), styrene trimer (PS), and 4-phenyl-4-pentenylonitrile (ABS) in polymer mixed standard S are represented by a matrix S (S = [0.6464,0.3808,0.02105]), and their contribution from mutual interference polymer is represented by matrix Y (Y = [1,0.2328,1.5242;0,1,6.3122;0,0,1]). The reconstructed chromatographic peak matrix X (X = [0.5563, 0.2479, 0.0210]) was obtained by solving the matrix Y and matrix S. By applying the algorithm to each mixed standard, the model fit was evaluated ($R^2$ = 0.98) and a calibration curve of PVC obtained ($R^2$ = 0.98). Finally, the reconstructed chromatographic peak matrix of Xsample (Xsample = [0.0322, 0.0115, 0.0004]) was determined and its PVC content (0.2007 μg) calculated.

## 2.5 Pretreatment Development and Condition Optimization

The digestion procedure (Figure S1-A) for organic matter removal was similar to our previous black carbon analysis of ambient aerosols in a high-pressure reactor.[58,59] The procedure offers the advantage of minimizing the influence of background contamination. Firstly, the samples and 2 mL digestion solution were added to the ampoules. The ampoules were sealed and placed into a 100-mL Teflon-lined stainless steel reaction vessel, which was then placed in an oven for heating. Subsequently, the ampoules were removed from the reaction vessel when it had cooled completely. The samples were transferred from the ampoules to glass fiber filters by a suction filtration system (Figure S1-B). Finally, the filters were used as carriers for collecting and introducing the MNPs from the samples to the pyrolyzer after freeze-drying. Each sample was represented by nine equal circles evenly cut from their corresponding collected filters (Figure S1-C) to reduce the limited loading volume of the pyrolysis cup and potentially inhomogeneous distribution of MNPs in $PM_{2.5}$ samples.[21,22]

To maximize organic matter removal and polymer recovery, pretreatment conditions, including filter type, digestion solution, digestion temperature, digestion time, and digestion solution concentration, were investigated. Three commonly used filters, including a glass fiber filter (GFF, 0.7 μm), polycarbonate track-etched filter (PCT, 0.4 μm), and anopore filter (AAO, 0.02 μm), were evaluated. The pyrolysis products of d-PS differed from non-deuterated PS in that they can effectively exclude contamination interference. Therefore, d-PS (0.25 μg) was spiked into the ultrapure water and passed through each filter via the filtration system to assess retention capability for MNPs.

In the digestion experiments, widely used acid and oxidant digestion methods were employed for organic matrix removal. Inorganic nitric acid ($HNO_3$, 65%), organic trifluoroacetic acid (TFA, 99%), and hydrogen peroxide ($H_2O_2$, 30%) were chosen as digestion solutions. Lignin, cellulose, and hemicellulose were treated to assess the efficiency of the digestion solution because they are naturally abundant and stable organic compounds,[60,61] and their pyrolysis products are similar to MNPs.[41,42] A

commercially mixed MNP standard was added into 2.0 mL of various digestion solution concentrations under different digestion temperatures (60–100°C, with intervals of 20°C) for varying periods of time (2–8 h, with intervals of 2 h). The optimal digestion parameters were determined by assessing both the recovery for MNPs and the removal of organic matter. The recovery was calculated using Eq. 2:

$$Recovery = \frac{m_d}{m_o} \times 100\% \quad \text{(Eq.2)}$$

where $m_d$ (μg) represents the detected mass of MNPs in the spiked samples after digestion, and $m_o$ (μg) represents the theoretical mass of MNPs initially spiked into the samples.

### 2.6 $PM_{2.5}$ Sample Collection

Sampling was conducted in November 2023 at an urban site in Guangzhou (Guangzhou Institute of Geochemistry, 23.149°N, 113.358°E). Ten $PM_{2.5}$ samples were collected on quartz fiber filters (QFF, 20.3 × 25.4 $cm^2$; Munktell) for 24 h, using a high-volume air sampler (Minya Instruments Co., Guangzhou, China.) at a flow rate of 1 $m^3$/min (Table S4). The filters were baked overnight at 450°C before use. After sampling, the filters were wrapped in prebaked aluminum foil, sealed, and stored in a −20°C freezer.

### 2.7 Quality Assurance and Quality Control

To avoid cross-contamination of plastic materials, the sampler is devoid of any plastic components, and plastic products were entirely avoided throughout both the sampling and laboratory operations. Cotton lab coats and vinyl gloves were used. Sample transfer was conducted using stainless steel tweezers. To minimize possible contamination on glass products, the GFF and all glass vessels were subjected to 6 h at 450°C, followed by wrapping in aluminum foil. Pure water and $HNO_3$ were prefiltered through 0.7 μm GFF filters and stored in glass containers. To check for plastic contamination from sampling and laboratory operations, field blanks were collected every three samples, and laboratory procedural blanks were included in each batch of sample pretreatments.

The same conditions for pretreatment and instrumental methods were applied to both the blanks and samples. To ensure analytical reliability, instrumental blanks were measured after every five samples, and instrument quality controls were conducted every five samples. Additionally, before sample loading, the pyrolysis cup was preheated using a flame gun. The limit of detection (LOD) and the limit of quantification (LOQ) were defined as the mass value corresponding to three times and 10 times the signal-to-noise ratio, respectively (Table S5). Background contamination in the procedure and field blanks was considered negligible (0.18 ± 0.11 μg/filter, n = 6) compared with real samples (mostly higher than 5.0 μg/filter).

# 3. Results and Discussion

## 3.1 Internal Interference among Polymers

The extracted ion chromatograms for all selected quantitative products (Table S2) from each individual polymer standard is illustrated in Figures S2–S5. The obvious peak of quantitative products for ABS, PE, PC, PMMA, and PP is exclusively observed in their respective polymer standard, indicating that those quantitative products are highly specific without any interference from other polymers (Figure S2).

However, in Figure S3, a distinct indene peak is consistently present in PVC, PS, and ABS standards, with a more intense indene peak in the PS standard than in the PVC standard. This suggests that the selection of indene as a quantitative product for PVC can be influenced by the presence of PS and ABS in a sample, leading to a potential overestimation of PVC content. Similarly, the benzene peak was identified in the PVC, PS, ABS, and PE standards in addition to the PET standard (Figure S4), indicating the co-generation of benzene from those five polymers. It is worth noting that the intensity of the benzene peak in the PET standard, with the same mass, was much higher than that in the PVC standard. This implies that using benzene as a PVC quantitative product could lead to significant overestimation, particularly with the reported high abundance of PET present in the environment.[49,62] Additionally, the presence of styrene trimer was

also detected in the ABS standard, which can be attributed to ABS being a copolymer of PS with the same monomer (Figure S5). The chosen quantitative products for PVC, PET, and PS are regarded as nonspecific and suffer interference from other polymers. Therefore, our chromatographic peak reconstruction algorithm was employed to construct the calibration and quantify the three polymers in our samples.

### 3.2 Quantification Procedure Performance

As shown in Table S5, the calibration curves were constructed using five mass gradients of mixed polymer standards covering eight polymers within the range of 0.2–20.0 μg. In addition, five single polymer standards (PE, PET, PVC, PS, and ABS) that contribute to the generation of nonspecific products were also analyzed for chromatographic peak reconstruction. Great linearity (>0.9) was observed in all source contribution equations for nonspecific products (Table S6), further confirming the assumption of a constant generation rate for pyrolysis products.

The calibration curves of the eight polymers showed great linearity with determination coefficients of $R^2 \geq 0.98$ (Table S5). The stability of the analysis was assessed through a triplicate analysis of the lowest calibration point. The response factor of each polymer displayed low relative standard deviations (<10%; Table S7), indicating stability of the instrumental method and repeatability of the polymer mixed standard. Moreover, this study achieved a relatively low LOD for eight polymers with a range of 0.002–0.009 μg, compared with the reported range of 0.001 to 0.05 μg in the literature.[37,49,63] These results suggest that our method is suitable for the detection of trace MNPs in $PM_{2.5}$.

Eight commercially mixed MNP standard samples were analyzed to evaluate the accuracy of our proposed quantification procedure. The mean determining accuracy of the five polymers ranged from 67 ± 11% (PC, n = 8) to 101 ± 10% (PE, n = 8) (Figure 3), indicating high precision in the calibration curves and feasibility in reducing the co-pyrolysis effect in a MNPs mixture. The relatively low accuracy of PC was likely attributed to the poor response of its quantitative product and its lower concentration in

the commercial MNPs standard, which was at least two times less than other polymers. The calculated masses of PS, PVC, and PET were quantified by applying the chromatographic peak reconstruction, and the results are presented in Figure 3 and Table S8. The calculated masses of PS, PVC, and PET were close to the expected masses, with an accuracy ranging from 64% to 132%, and a mean accuracy exceeding 89% for these polymers. The high accuracy demonstrates the effectiveness of the proposed algorithm in reducing the mutual interference of polymers in MNP mixtures. Additionally, the high determining accuracy of ABS (90 ± 11%, n = 8) and PS (89 ± 22%, n = 8) suggests that the proposed algorithm can effectively differentiate between copolymers.

To our knowledge, this method represents a pioneering approach capable of effectively resolving quantitative interference among polymers in MNP mixtures resulting from the selection of nonspecific pyrolysis products. Furthermore, in contrast to traditional methods that typically rely on tetramethylammonium hydroxide (TMAH) for benzoic acid derivatization to enhance PET quantification,[28,64] this study also achieved accurate quantification of PET without derivatization. Moreover, this method has shown capability, for the first time, to differentiate copolymers based on Py-GC/MS, such as ABS and PS.

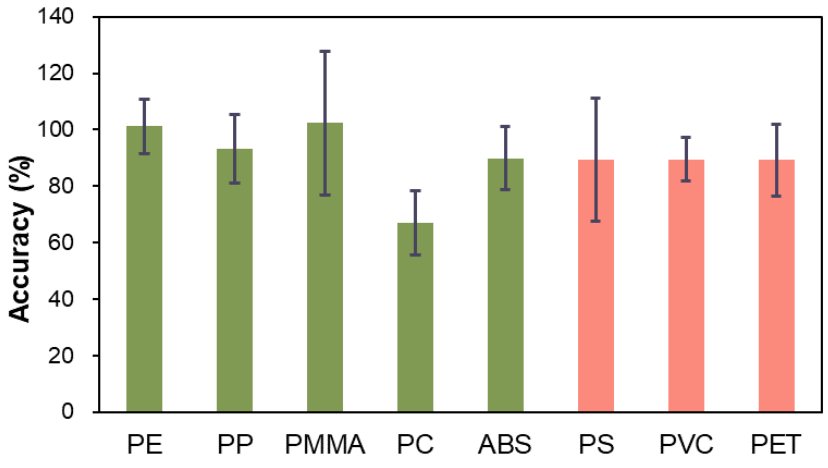


Figure 3. The mean accuracy of each polymer by the proposed quantification procedure in eight commercially mixed MNP standards. The accuracy was calculated according to Eq. 1. Error bars indicate the standard deviations. The green bar represents the mean accuracy of polymers

unaffected by internal interference, while the orange bar denotes polymers affected by internal interference.

### 3.3 Optimization of the Pretreatment Procedure

#### 3.3.1 Filter Selection

The suitability of three commonly used filters (GFF, PCTE, and AAO) for MNPs analysis was evaluated via d-PS intensity in the chromatogram of those spiked filter samples. Suitable filters were identified as those showing similar responses (with a difference in peak area ≤20%) to the d-PS standard sample of equivalent mass. The chromatograms of spiked filter samples and a d-PS standard sample (0.25 μg) are shown in Figure S6. The results showed a comparable intensity of quantitative ion (styrene-$d_7$, m/z 111) of d-PS in both the PCTE (peak area: $3.9 \times 10^6$) and GFF (peak area: $4.0 \times 10^6$) samples, as well as the d-PS standard sample (peak area: $4.2 \times 10^6$). This finding indicates that both PCTE and GFF effectively retained MNPs during filtration. Conversely, the peak area of styrene-$d_7$ in the AAO filter sample (peak area: $6.1 \times 10^5$) is lower than that of the d-PS standard sample. This difference can be attributed to the single-layer structure and smooth surface of an AAO filter, making it hard to retain MNPs. Furthermore, a high baseline and elevated intensity of PC was observed in the PCTE filter sample, indicating extra interference from this organic filter (Figure S6-A). As a result, the GFF was selected to collect the MNPs for pyrolysis analysis.

#### 3.3.2 Digestion Solution Selection

Excess mixed organic matter (1.5 mg), consisting of lignin, cellulose, and hemicellulose, was used as a model to evaluate the removal efficiency of different digestion solutions. The chromatograms of the procedural blank samples were compared with those of mixed organic matter samples digested with three solutions (6 h at 100℃ in equal proportions of $H_2O_2$, TFA, and $HNO_3$) to determine the most effective digestion solution (Figure S7). The total ion chromatogram for the $H_2O_2$ (Figure S7-A) and TFA (Figure S7-B) groups showed a high baseline and intensity of characteristic compounds of MNPs, suggesting insufficient removal of organic matter. In contrast, the total ion

chromatogram for the $HNO_3$ group shows an apparent reduction in both baseline and noise peaks, similar to the procedural blank sample (Figure S7-C). In addition, the extracted ion chromatograms of all polymers for the $HNO_3$ group maintained consistently low intensity consistent with the procedure blank, indicating the complete removal of organic matter (Figure S8 and Figure S9).

$H_2O_2$ destroys the structure of organic compounds, such as lignin, through oxidation,[65] thereby achieving removing organic matter. However, $H_2O_2$ treatment takes a relatively long time for effective organic matter removal,[66,67] as confirmed by the results of this study. Similarly, TFA effectively reduces the crystallinity of organic compounds like cellulose, but its degradation efficiency for organic compounds is limited.[68] $HNO_3$, known for its strong oxidative properties, has been shown in previous studies to effectively oxygenolyze polyaromatic organic matter from the atmosphere,[58,59] and this study also found it can completely remove target organic matter. During the same digestion conditions in this study, $HNO_3$ was identified as the most effective digestion solution and was used for digestion.

### 3.3.3 Digestion Parameter Optimization

To achieve the optimum recovery of MNPs, the key digestion parameters, including temperature, time, and $HNO_3$ concentration, were investigated. The digestion temperature was optimized within a range of 60°C to 100°C for 6 h and 2 mL 65% $HNO_3$. Figure 4-A shows a significant increase in all MNP recoveries after temperatures were reduced to 80°C from 100°C with the recoveries for PE, PP, PC, and PVC exceeding 60%, indicating the destructive effects of a digestion temperature of 100°C. When further decreasing the digestion temperature from 80°C to 60°C, minimal changes were observed in the recoveries of PE, PP, PC, and PVC. However, substantial enhancements (40%) were detected in the recoveries of ABS, PS, PMMA, and PET. Additionally, as shown in Figure S10, the organic matter mixture was eliminated even at digestion temperatures of 60°C. Hence, a temperature of 60°C was adopted for digestion.

The digestion time was optimized in the range of 2–6 h, using a digestion temperature of 60°C and 2 mL 65% $HNO_3$. As shown in Figure 4-B, the recoveries of most MNPs showed an apparent increase ranging from 7% (PMMA) to 17% (PVC) when the time was shortened to 4 h. When the digestion time was further reduced to 2 h, no obvious changes were observed in the recoveries of MNPs except for PET, which exhibited a 35% recovery increase. Furthermore, Figure S11 shows a similar total ion chromatogram with the procedure blank, suggesting that the organic matter mixture can be eliminated after 2 h of digestion. Therefore, a 2 h digestion time was optimal and used in the following experiments.

The effects of $HNO_3$ concentration on MNP recovery were investigated after digestion for 2 h at 60°C. Organic matter removal showed a clear chromatogram at 32% $HNO_3$ (Figure S12-B), but impure peaks increased at 26% $HNO_3$ (Figure S12-A), indicating insufficient removal below this concentration. Therefore, only the recoveries of the 32% $HNO_3$ group were used for comparison with the 65% $HNO_3$ group. As illustrated in Figure 4-C, the recovery of all MNPs increased with decreasing $HNO_3$ concentration from 65% to 32%, and the recoveries of PS, ABS, and PC increased most significantly (>60%). Hence, we concluded that the optimal concentration for $HNO_3$ was 32%. Under these optimized conditions, the average recovery for PE, PP, PS, ABS, PMMA, PC, PVC, and PET were 97 ± 14%, 89 ± 7%, 63 ± 2%, 64 ± 8%, 70 ± 7%, 87 ± 14%, 84 ± 25%, and 92 ± 14%, respectively.

To verify the effectiveness of the proposed digestion method in real $PM_{2.5}$ samples, a blank matrix experiment was conducted by spiking the commercial MNPs standards into prebaked QFF filters. As shown in Figure 4-D, the recoveries of all MNPs remained within satisfactory ranges, comparable to the blank recoveries observed during pretreatment. Recoveries ranged from 60 ± 7% (PMMA) to 98 ± 7% (PE), indicating little matrix effect on the proposed method. In conclusion, compared with other $HNO_3$ digestion methods,[69,70] this proposed method can effectively remove interference from organic matrices in a shorter time (2 h) and achieve a relatively high recovery rate of

MNPs, making it applicable to atmospheric $PM_{2.5}$.

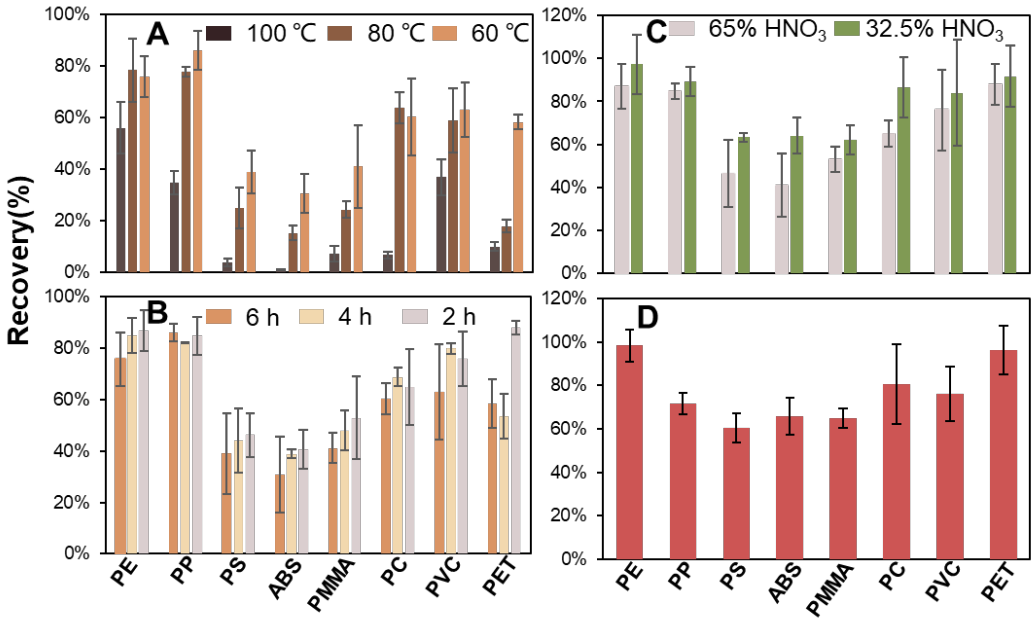


Figure 4. (A) Mean recoveries (n = 6) of various MNPs at different temperatures for 6 h and 2 mL 65% $HNO_3$. (B) Mean recoveries (n = 6) at different durations of digestion at 60°C with 2 mL 65% $HNO_3$. (C) Mean recoveries (n = 6) under different concentrations of $HNO_3$ at 60°C over 2 h. (D) Mean recoveries (n = 6) of various MNPs in the matrix spike experiment.

### 3.4 Demonstration in $PM_{2.5}$ Samples

This proposed digestion method and chromatography reconstruction procedure were used to quantify MNPs in urban Guangzhou $PM_{2.5}$ samples. Each sample consisted of nine circles (1 cm diameter each) cut from their filter, representing a sampling volume of 30.3 $m^3$. To evaluate the reproducibility of this sampling method, five replicates from the same sample were analyzed (Figure S13). The total concentration of MNPs ($\sum_8$MNPs) across the five replicates shows consistency, with a relative standard deviation of less than 12% (Figure S14), indicating that the sampling method is both representative and reliable.

Four polymers, PE, PMMA, PVC, and PET, were detected in all $PM_{2.5}$ samples. However, PP, PS, and PC were only detected in specific samples, with detection rates of 20%–90%. ABS was not observed in any samples, likely due to its propensity to accumulate in the larger aerodynamic diameter stage.[43] Total $\sum_8$MNPs concentrations

in $PM_{2.5}$ samples ranged from 99.7 to 982.8 ng / $m^3$ (Figure S15). As shown in Figure 5 and Figure S16, the MNPs in $PM_{2.5}$ were dominated by PE, PET, and PVC, accounting for 13%–80% (median 57%), 8%–83% (median 26%), and 2%–29% (median 12%), respectively. Their concentrations ranged from 19.1–661.3 ng/$m^3$ (median 98.5 ng/$m^3$) for PE, 8.2–393.4 ng/$m^3$ (median 61.5 ng/$m^3$; PET), to 2.3–133.2 ng/$m^3$ (median 22.2 ng/$m^3$ for PVC. In contrast, the concentrations of PMMA (0.3–40.8 ng/$m^3$), PP (not detectable to 16.0 ng/$m^3$), PC (not detectable to 6.2 ng/$m^3$), and PS (not detectable to 5.8 ng/$m^3$) were an order of magnitude lower than the dominant polymers, collectively constituting 1%–9% (median 6%) of the total concentrations.

Available data on the mass concentration of MNPs in the atmosphere are limited. To date, only six studies have reported their mass-based levels in atmospheric particulate matter, spanning aerodynamic diameters ranging from 1 to ≥10 μm.[20–23,5,49] A review of each target polymer's concentration is detailed in Table S9. Regarding individual polymer concentrations within $PM_{2.5}$, significant differences were observed. The mean concentration of PE in this study was found to be lower by two orders of magnitude compared with observations in Shanghai (4200 ng/$m^3$), yet three orders of magnitude higher than those reported across three Chinese cities ($6 \times 10^{-3}$ ng/$m^3$). Similarly, the mean concentrations of PVC and PS in this study were lower by 1–2 orders of magnitude than those observed in Shanghai (500 and 600 ng/$m^3$, respectively). However, the mean concentrations of PS and PP were 10 times and three times higher than that observed in Tokushima, Japan (0.38 and 1.75 ng/$m^3$, respectively). PET, PMMA, and PC were first detected in $PM_{2.5}$ in this study. The mean concentrations of PET and PMMA were found to be 10 times and two times higher, respectively, compared with those reported in $PM_{\geq 5\ \mu m}$ from the Swedish coastal region. In contrast, the mean level of PC was comparable to their reported values. These results suggest a higher level of MNPs in urban $PM_{2.5}$ samples.

In terms of MNP composition, our findings were similar to previous studies that PE (20%–27%) and PET (16%–75%) were the primary components of MNPs in urban

atmospheric total suspended particulate matter (TSP) in China.[9,62,71,72] However, the average proportion of PE and PVC identified in this study was twice as high as previously reported in urban TSP samples (27% for PE and 7% for PVC),[62] indicating their high accumulation in $PM_{2.5}$. Conversely, other polymers (PS, PP, PMMA, and PC) identified in higher proportions in previous works[9,49,62] were found to contribute a negligible proportion to our samples. The differences between our results and the literature may be attributed to factors including differences in sampling locations across studies as well as different analytical methodologies applied. Thus, a standard methodology is needed for further research.

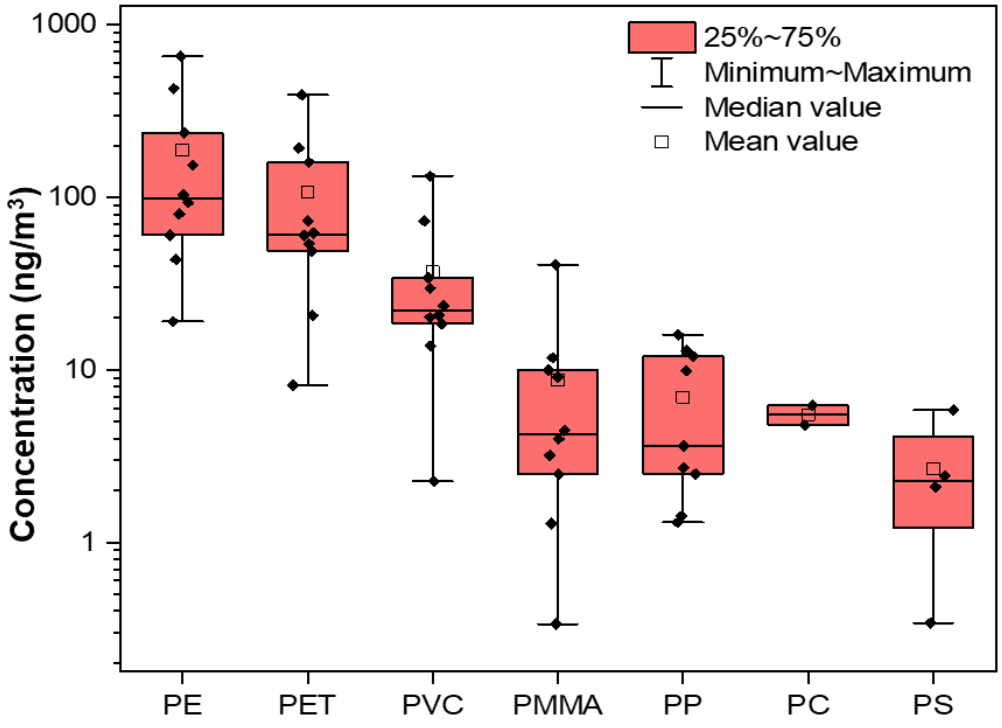


Figure 5. Concentrations of seven types of detected polymer in 10 $PM_{2.5}$ samples from urban Guangzhou (China).

### 3.5 Limitations and Environmental Implications

Previous studies have found that $HNO_3$ has a destructive effect on low pH-tolerant polymers (such as PS and PE), but following digestion parameter optimization, the $HNO_3$ digestion method proposed in this study achieved acceptable recovery (60% –

98%) for the eight target polymers, without significant underestimation of MNP concentrations. Moreover, the chromatographic baseline of processed samples shown in Py-GC-MS remains low and clear, aiding in enhancing quantitative accuracy and partly offsetting the uncertainty resulting from pretreatment losses. This study also found that under the same digestion conditions (time and temperature), $H_2O_2$ is less efficient than $HNO_3$ in removing organic matter. Therefore, when dealing with large batches of samples or samples with high organic matter content (such as soil and sediment), the proposed $HNO_3$ digestion is more advantageous.

The chromatographic peak reconstruction procedure proposed in this study can effectively reduce internal interference among polymers and accurately differentiate copolymers (average accuracy >89%), showing great advantages when conducting risk assessment of MNPs. Currently, most studies that assess exposure risk posed by MNPs are calculated via MNP mass concentrations converted by number concentration using a mathematical model, which induces a high level of uncertainty. Due to the diversity in copolymer structures, absorption and accumulation of individual copolymers in organisms would vary greatly, potentially resulting in different adverse effects.[74] We conducted the first investigation into eight major polymers in urban $PM_{2.5}$ samples, revealing that Guangzhou $PM_{2.5}$ is primarily composed of PE, PET, and PVC (>90% of the total polymers). As current toxicity tests mainly use PS or PE as model polymers, this could potentially underestimate the risk posed by MNPs.[15,75–77]

Despite the extensive methodological research on MNPs, there is still a lack of unified standard analytical methods for atmospheric MNPs.[79] Hence, it is challenging to compare regional differences in MNP occurrences and compositions. There can be variations of three to six orders of magnitude between the results of this study and other published research even for the same city. The International Organization for Standardization has issued basic principles for sampling, sample preparation, and detection of microplastics in the atmosphere.[80] The pretreatment and quantification methods proposed in this study provide beneficial supplements and references for

implementation under those principles. Furthermore, to enhance the reliability and reproducibility of MNPs determination, it is essential to conduct an inter-laboratory cross-validation study for analytical methods. Finally, a standardized international monitoring network should be developed for better understanding of the sources, transport, and impact of atmospheric MNPs, thereby providing scientific evidence for the development of effective protection and management measures.

## Supporting Information

Detailed information regarding chemicals, samples, instrumental methods, calibration standards, calibration curves, and additional results.

## References


(1) Ivleva, N. P. Chemical Analysis of Microplastics and Nanoplastics: Challenges, Advanced Methods, and Perspectives. *Chem. Rev.* **2021**, *121* (19), 11886–11936. https://doi.org/10.1021/acs.chemrev.1c00178.

(2) Hartmann, N. B.; Hüffer, T.; Thompson, R. C.; Hassellöv, M.; Verschoor, A.; Daugaard, A. E.; Rist, S.; Karlsson, T.; Brennholt, N.; Cole, M.; Herrling, M. P.; Hess, M. C.; Ivleva, N. P.; Lusher, A. L.; Wagner, M. Are We Speaking the Same Language? Recommendations for a Definition and Categorization Framework for Plastic Debris. *Environ. Sci. Technol.* **2019**, *53* (3), 1039–1047. https://doi.org/10.1021/acs.est.8b05297.

(3) Trainic, M.; Flores, J. M.; Pinkas, I.; Pedrotti, M. L.; Lombard, F.; Bourdin, G.; Gorsky, G.; Boss, E.; Rudich, Y.; Vardi, A.; Koren, I. Airborne Microplastic Particles Detected in the Remote Marine Atmosphere. *Commun. Earth Environ.* **2020**, *1* (1), 1–9. https://doi.org/10.1038/s43247-020-00061-y.

(4) Allen, S.; Allen, D.; Phoenix, V. R.; Le Roux, G.; Durántez Jiménez, P.; Simonneau, A.; Binet, S.; Galop, D. Atmospheric Transport and Deposition of Microplastics in a Remote Mountain Catchment. *Nat. Geosci.* **2019**, *12* (5), 339–344. https://doi.org/10.1038/s41561-019-0335-5.

(5) Goßmann, I.; Herzke, D.; Held, A.; Schulz, J.; Nikiforov, V.; Georgi, C.; Evangeliou, N.; Eckhardt, S.; Gerdts, G.; Wurl, O.; Scholz-Böttcher, B. M. Occurrence and Backtracking of Microplastic Mass Loads Including Tire Wear

Particles in Northern Atlantic Air. *Nat. Commun.* **2023**, *14* (1), 3707. https://doi.org/10.1038/s41467-023-39340-5.

(6) Luo, D.; Wang, Z.; Liao, Z.; Chen, G.; Ji, X.; Sang, Y.; Qu, L.; Chen, Z.; Wang, Z.; Dahlgren, R. A.; Zhang, M.; Shang, X. Airborne Microplastics in Urban, Rural and Wildland Environments on the Tibetan Plateau. *J. Hazard. Mater.* **2024**, *465*, 133177. https://doi.org/10.1016/j.jhazmat.2023.133177.

(7) Bianco, A.; Passananti, M. Atmospheric Micro and Nanoplastics: An Enormous Microscopic Problem. *Sustainability* **2020**, *12* (18), 7327. https://doi.org/10.3390/su12187327.

(8) Liu, P.; Shao, L.; Zhang, Y.; Silvonen, V.; Oswin, H.; Cao, Y.; Guo, Z.; Ma, X.; Morawska, L. Atmospheric Microplastic Deposition Associated with GDP and Population Growth: Insights from Megacities in Northern China. *J. Hazard. Mater.* **2024**, *469*, 134024. https://doi.org/10.1016/j.jhazmat.2024.134024.

(9) Wang, X.; Li, C.; Liu, K.; Zhu, L.; Song, Z.; Li, D. Atmospheric Microplastic over the South China Sea and East Indian Ocean: Abundance, Distribution and Source. *J. Hazard. Mater.* **2020**, *389*, 121846. https://doi.org/10.1016/j.jhazmat.2019.121846.

(10) Yuan, Z.; Pei, C.; Li, H.; Lin, L.; Liu, S.; Hou, R.; Liao, R.; Xu, X. Atmospheric Microplastics at a Southern China Metropolis: Occurrence, Deposition Flux, Exposure Risk and Washout Effect of Rainfall. *Sci. Total Environ.* **2023**, *869*, 161839. https://doi.org/10.1016/j.scitotenv.2023.161839.

(11) Huang, Y.; He, T.; Yan, M.; Yang, L.; Gong, H.; Wang, W.; Qing, X.; Wang, J. Atmospheric Transport and Deposition of Microplastics in a Subtropical Urban Environment. *J. Hazard. Mater.* **2021**, *416*, 126168. https://doi.org/10.1016/j.jhazmat.2021.126168.

(12) Wright, S. L.; Kelly, F. J. Plastic and Human Health: A Micro Issue? *Environ. Sci. Technol.* **2017**, *51* (12), 6634–6647. https://doi.org/10.1021/acs.est.7b00423.

(13) Vethaak, A. D.; Legler, J. Microplastics and Human Health. *Science.* **2021**, *371* (6530), 672–674. https://doi.org/10.1126/science.abe5041.

(14) Sridharan, S.; Kumar, M.; Singh, L.; Bolan, N. S.; Saha, M. Microplastics as an Emerging Source of Particulate Air Pollution: A Critical Review. *J. Hazard. Mater.* **2021**, *418*, 126245. https://doi.org/10.1016/j.jhazmat.2021.126245.

(15) Sun, H.; Yang, B.; Zhu, X.; Li, Q.; Song, E.; Song, Y. Oral Exposure of Polystyrene Microplastics and Doxycycline Affects Mice Neurological Function *via* Gut Microbiota Disruption: The Orchestrating Role of Fecal Microbiota

Transplantation. *J. Hazard. Mater.* **2024**, *467*, 133714. https://doi.org/10.1016/j.jhazmat.2024.133714.

(16) Wang, H.; Wang, Y.; Wang, Q.; Lv, M.; Zhao, X.; Ji, Y.; Han, X.; Wang, X.; Chen, L. The Combined Toxic Effects of Polyvinyl Chloride Microplastics and Di(2-Ethylhexyl) Phthalate on the Juvenile Zebrafish (*Danio Rerio*). *J. Hazard. Mater.* **2022**, *440*, 129711. https://doi.org/10.1016/j.jhazmat.2022.129711.

(17) Marfella, R.; Prattichizzo, F.; Sardu, C.; Fulgenzi, G.; Graciotti, L.; Spadoni, T.; D'Onofrio, N.; Scisciola, L.; La Grotta, R.; Frigé, C.; Pellegrini, V.; Municinò, M.; Siniscalchi, M.; Spinetti, F.; Vigliotti, G.; Vecchione, C.; Carrizzo, A.; Accarino, G.; Squillante, A.; Spaziano, G.; Mirra, D.; Esposito, R.; Altieri, S.; Falco, G.; Fenti, A.; Galoppo, S.; Canzano, S.; Sasso, F. C.; Matacchione, G.; Olivieri, F.; Ferraraccio, F.; Panarese, I.; Paolisso, P.; Barbato, E.; Lubritto, C.; Balestrieri, M. L.; Mauro, C.; Caballero, A. E.; Rajagopalan, S.; Ceriello, A.; D'Agostino, B.; Iovino, P.; Paolisso, G. Microplastics and Nanoplastics in Atheromas and Cardiovascular Events. *N. Engl. J. Med.* **2024**, *390* (10), 900–910. https://doi.org/10.1056/NEJMoa2309822.

(18) Sridharan, S.; Kumar, M.; Singh, L.; Bolan, N. S.; Saha, M. Microplastics as an Emerging Source of Particulate Air Pollution: A Critical Review. *J. Hazard. Mater.* **2021**, *418*, 126245. https://doi.org/10.1016/j.jhazmat.2021.126245.

(19) Cohen, A. J.; Brauer, M.; Burnett, R.; Anderson, H. R.; Frostad, J.; Estep, K.; Balakrishnan, K.; Brunekreef, B.; Dandona, L.; Dandona, R.; Feigin, V.; Freedman, G.; Hubbell, B.; Jobling, A.; Kan, H.; Knibbs, L.; Liu, Y.; Martin, R.; Morawska, L.; Pope, C. A.; Shin, H.; Straif, K.; Shaddick, G.; Thomas, M.; van Dingenen, R.; van Donkelaar, A.; Vos, T.; Murray, C. J. L.; Forouzanfar, M. H. Estimates and 25-Year Trends of the Global Burden of Disease Attributable to Ambient Air Pollution: An Analysis of Data from the Global Burden of Diseases Study 2015. *The Lancet.* **2017**, *389* (10082), 1907–1918. https://doi.org/10.1016/S0140-6736(17)30505-6.

(20) Mizuguchi, H.; Takeda, H.; Kinoshita, K.; Takeuchi, M.; Takayanagi, T.; Teramae, N.; Pipkin, W.; Matsui, K.; Watanabe, A.; Watanabe, C. Direct Analysis of Airborne Microplastics Collected on Quartz Filters by Pyrolysis-Gas Chromatography/Mass Spectrometry. *J. Anal. Appl. Pyrolysis.* **2023**, *171*, 105946. https://doi.org/10.1016/j.jaap.2023.105946.

(21) Luo, P.; Bai, M.; He, Q.; Peng, Z.; Wang, L.; Dong, C.; Qi, Z.; Zhang, W.; Zhang, Y.; Cai, Z. A Novel Strategy to Directly Quantify Polyethylene Microplastics in PM2.5 Based on Pyrolysis-Gas Chromatography–Tandem Mass Spectrometry. *Anal. Chem.* **2023**, *95* (7), 3556–3562. https://doi.org/10.1021/acs.analchem.2c05477.

(22) Sheng, X.; Lai, Y.; Yu, S.; Li, Q.; Zhou, Q.; Liu, J. Quantitation of Atmospheric Suspended Polystyrene Nanoplastics by Active Sampling Prior to Pyrolysis–Gas Chromatography–Mass Spectrometry. *Environ. Sci. Technol.* **2023**. https://doi.org/10.1021/acs.est.3c02299.

(23) Chen, Y.; Jing, S.; Wang, Y.; Song, Z.; Xie, L.; Shang, X.; Fu, H.; Yang, X.; Wang, H.; Wu, M.; Chen, Y.; Li, Q.; Zhang, Y.; Wang, W.; Zhang, L.; Wang, R.; Fang, M.; Zhang, Y.; Li, W.; Zhao, D.; Li, C.; Rudich, Y.; Wang, L.; Zhang, R.; Liu, W.; Wanger, T. C.; Yu, S.; Chen, J. Quantification and Characterization of Fine Plastic Particles as Considerable Components in Atmospheric Fine Particles. *Environ. Sci. Technol.* **2024**. https://doi.org/10.1021/acs.est.3c06832.

(24) Primpke, S.; Wirth, M.; Lorenz, C.; Gerdts, G. Reference Database Design for the Automated Analysis of Microplastic Samples Based on Fourier Transform Infrared (FTIR) Spectroscopy. *Anal. Bioanal. Chem.* **2018**, *410* (21), 5131–5141. https://doi.org/10.1007/s00216-018-1156-x.

(25) Jung, S.; Cho, S.-H.; Kim, K.-H.; Kwon, E. E. Progress in Quantitative Analysis of Microplastics in the Environment: A Review. *Chem. Eng. J.* **2021**, *422*, 130154. https://doi.org/10.1016/j.cej.2021.130154.

(26) Primpke, S.; Christiansen, S. H.; Cowger, W.; De Frond, H.; Deshpande, A.; Fischer, M.; Holland, E. B.; Meyns, M.; O'Donnell, B. A.; Ossmann, B. E.; Pittroff, M.; Sarau, G.; Scholz-Böttcher, B. M.; Wiggin, K. J. Critical Assessment of Analytical Methods for the Harmonized and Cost-Efficient Analysis of Microplastics. *Appl. Spectrosc.* **2020**, *74* (9), 1012–1047. https://doi.org/10.1177/0003702820921465.

(27) Xu, Y.; Ou, Q.; van der Hoek, J. P.; Liu, G.; Lompe, K. M. Photo-Oxidation of Micro- and Nanoplastics: Physical, Chemical, and Biological Effects in Environments. *Environ. Sci. Technol.* **2024**, *58* (2), 991–1009. https://doi.org/10.1021/acs.est.3c07035.

(28) Fischer, M.; Scholz-Böttcher, B. M. Simultaneous Trace Identification and Quantification of Common Types of Microplastics in Environmental Samples by Pyrolysis-Gas Chromatography–Mass Spectrometry. *Environ. Sci. Technol.* **2017**, *51* (9), 5052–5060. https://doi.org/10.1021/acs.est.6b06362.

(29) Fan, W.; Salmond, J. A.; Dirks, K. N.; Cabedo Sanz, P.; Miskelly, G. M.; Rindelaub, J. D. Evidence and Mass Quantification of Atmospheric Microplastics in a Coastal New Zealand City. *Environ. Sci. Technol.* **2022**, *56* (24), 17556–17568. https://doi.org/10.1021/acs.est.2c05850.

(30) Li, Q.; Bai, Q.; Sheng, X.; Li, P.; Zheng, R.; Yu, S.; Liu, J. Influence of Particle Characteristics, Heating Temperature and Time on the Pyrolysis Product

667 Distributions of Polystyrene Micro- and Nano-Plastics. *J. Chromatogr. A* **2022**,
668 *1682*, 463503. https://doi.org/10.1016/j.chroma.2022.463503.

669 (31) Xu, Y.; Ou, Q.; Jiao, M.; Liu, G.; van der Hoek, J. P. Identification and
670 Quantification of Nanoplastics in Surface Water and Groundwater by Pyrolysis
671 Gas Chromatography–Mass Spectrometry. *Environ. Sci. Technol.* **2022**, *56* (8),
672 4988–4997. https://doi.org/10.1021/acs.est.1c07377.

673 (32) Fischer, M.; Scholz-Böttcher, B. M. Microplastics Analysis in Environmental
674 Samples – Recent Pyrolysis-Gas Chromatography-Mass Spectrometry Method
675 Improvements to Increase the Reliability of Mass-Related Data. *Anal. Methods.*
676 **2019**, *11* (18), 2489–2497. https://doi.org/10.1039/C9AY00600A.

677 (33) Rødland, E. S.; Samanipour, S.; Rauert, C.; Okoffo, E. D.; Reid, M. J.; Heier, L.
678 S.; Lind, O. C.; Thomas, K. V.; Meland, S. A Novel Method for the Quantification
679 of Tire and Polymer-Modified Bitumen Particles in Environmental Samples by
680 Pyrolysis Gas Chromatography Mass Spectroscopy. *J. Hazard. Mater.* **2022**, *423*,
681 127092. https://doi.org/10.1016/j.jhazmat.2021.127092.

682 (34) Kamp, J.; Dierkes, G.; Schweyen, P. N.; Wick, A.; Ternes, T. A. Quantification of
683 Poly(Vinyl Chloride) Microplastics via Pressurized Liquid Extraction and
684 Combustion Ion Chromatography. *Environ. Sci. Technol.* **2023**, *57* (12), 4806–
685 4812. https://doi.org/10.1021/acs.est.2c06555.

686 (35) Hermabessiere, L.; Himber, C.; Boricaud, B.; Kazour, M.; Amara, R.; Cassone,
687 A.-L.; Laurentie, M.; Paul-Pont, I.; Soudant, P.; Dehaut, A.; Duflos, G.
688 Optimization, Performance, and Application of a Pyrolysis-GC/MS Method for
689 the Identification of Microplastics. *Anal. Bioanal. Chem.* **2018**, *410* (25), 6663–
690 6676. https://doi.org/10.1007/s00216-018-1279-0.

691 (36) Gregoris, E.; Gallo, G.; Rosso, B.; Piazza, R.; Corami, F.; Gambaro, A.
692 Microplastics Analysis: Can We Carry out a Polymeric Characterisation of
693 Atmospheric Aerosol Using Direct Inlet Py-GC/MS? *J. Anal. Appl. Pyrolysis.*
694 **2023**, *170*, 105903. https://doi.org/10.1016/j.jaap.2023.105903.

695 (37) Goßmann, I.; Süßmuth, R.; Scholz-Böttcher, B. M. Plastic in the Air?! - Spider
696 Webs as Spatial and Temporal Mirror for Microplastics Including Tire Wear
697 Particles in Urban Air. *Sci. Total Environ.* **2022**, *832*, 155008.
698 https://doi.org/10.1016/j.scitotenv.2022.155008.

699 (38) Kaal, J.; Goñi-Urtiaga, A.; Wenig, P.; Veliu, M.; Moreno-Jiménez, E.; Plaza, C.;
700 Panettieri, M. Simultaneous Molecular Fingerprinting of Natural Organic Matter
701 and Synthetic Polymers (PE, PET, PP, PS and PVC) Using Analytical Pyrolysis.
702 *J. Anal. Appl. Pyrolysis.* **2023**, *175*, 106159.
703 https://doi.org/10.1016/j.jaap.2023.106159.

(39) La Nasa, J.; Biale, G.; Fabbri, D.; Modugno, F. A Review on Challenges and Developments of Analytical Pyrolysis and Other Thermoanalytical Techniques for the Quali-Quantitative Determination of Microplastics. *J. Anal. Appl. Pyrolysis* **2020**, *149*, 104841. https://doi.org/10.1016/j.jaap.2020.104841.

(40) Kebelmann, K.; Hornung, A.; Karsten, U.; Griffiths, G. Intermediate Pyrolysis and Product Identification by TGA and Py-GC/MS of Green Microalgae and Their Extracted Protein and Lipid Components. *Biomass Bioenergy.* **2013**, *49*, 38–48. https://doi.org/10.1016/j.biombioe.2012.12.006.

(41) Chen, H.; Rhoades, C. C.; Chow, A. T. Characteristics of Soil Organic Matter 14 Years after a Wildfire: A Pyrolysis-Gas-Chromatography Mass Spectrometry (Py-GC-MS) Study. *J. Anal. Appl. Pyrolysis.* **2020**, *152*, 104922. https://doi.org/10.1016/j.jaap.2020.104922.

(42) Girona-García, A.; Badía-Villas, D.; Jiménez-Morillo, N. T.; González-Pérez, J. A. Changes in Soil Organic Matter Composition after Scots Pine Afforestation in a Native European Beech Forest Revealed by Analytical Pyrolysis (Py-GC/MS). *Sci. Total Environ.* **2019**, *691*, 1155–1161. https://doi.org/10.1016/j.scitotenv.2019.07.229.

(43) Mizuguchi, H.; Takeda, H.; Kinoshita, K.; Takeuchi, M.; Takayanagi, T.; Teramae, N.; Pipkin, W.; Matsui, K.; Watanabe, A.; Watanabe, C. Direct Analysis of Airborne Microplastics Collected on Quartz Filters by Pyrolysis-Gas Chromatography/Mass Spectrometry. *J. Anal. Appl. Pyrolysis.* **2023**, *171*, 105946. https://doi.org/10.1016/j.jaap.2023.105946.

(44) Didyk, B. M.; Simoneit, B. R. T.; Alvaro Pezoa, L.; Luis Riveros, M.; Anselmo Flores, A. Urban Aerosol Particles of Santiago, Chile:: Organic Content and Molecular Characterization. *Atmos. Environ.* **2000**, *34* (8), 1167–1179. https://doi.org/10.1016/S1352-2310(99)00403-3.

(45) Hiranuma, N.; Möhler, O.; Yamashita, K.; Tajiri, T.; Saito, A.; Kiselev, A.; Hoffmann, N.; Hoose, C.; Jantsch, E.; Koop, T.; Murakami, M. Ice Nucleation by Cellulose and Its Potential Contribution to Ice Formation in Clouds. *Nat. Geosci.* **2015**, *8* (4), 273–277. https://doi.org/10.1038/ngeo2374.

(46) Matthias-Maser, S.; Jaenicke, R. The Size Distribution of Primary Biological Aerosol Particles with Radii > 0.2 Mm in an Urban/Rural Influenced Region. *Atmospheric Res.* **1995**, *39* (4), 279–286. https://doi.org/10.1016/0169-8095(95)00017-8.

(47) Matsueda, M.; Mattonai, M.; Iwai, I.; Watanabe, A.; Teramae, N.; Robberson, W.; Ohtani, H.; Kim, Y.-M.; Watanabe, C. Preparation and Test of a Reference Mixture of Eleven Polymers with Deactivated Inorganic Diluent for Microplastics Analysis

by Pyrolysis-GC–MS. *J. Anal. Appl. Pyrolysis.* **2021**, *154*, 104993. https://doi.org/10.1016/j.jaap.2020.104993.

(48) La Nasa, J.; Biale, G.; Mattonai, M.; Modugno, F. Microwave-Assisted Solvent Extraction and Double-Shot Analytical Pyrolysis for the Quali-Quantitation of Plasticizers and Microplastics in Beach Sand Samples. *J. Hazard. Mater.* **2021**, *401*, 123287. https://doi.org/10.1016/j.jhazmat.2020.123287.

(49) Goßmann, I.; Mattsson, K.; Hassellöv, M.; Crazzolara, C.; Held, A.; Robinson, T.-B.; Wurl, O.; Scholz-Böttcher, B. M. Unraveling the Marine Microplastic Cycle: The First Simultaneous Data Set for Air, Sea Surface Microlayer, and Underlying Water. *Environ. Sci. Technol.* **2023**, *57* (43), 16541–16551. https://doi.org/10.1021/acs.est.3c05002.

(50) Lauschke, T.; Dierkes, G.; Ternes, T. A. Challenges in the Quantification of Poly(Ethylene Terephthalate) Microplastics via Thermoanalytical Methods Posed by Inorganic Matrix Components. *J. Anal. Appl. Pyrolysis.* **2023**, *174*, 106108. https://doi.org/10.1016/j.jaap.2023.106108.

(51) Krauskopf, L.-M.; Hemmerich, H.; Dsikowitzky, L.; Schwarzbauer, J. Critical Aspects on Off-Line Pyrolysis-Based Quantification of Microplastic in Environmental Samples. *J. Anal. Appl. Pyrolysis.* **2020**, *152*, 104830. https://doi.org/10.1016/j.jaap.2020.104830.

(52) Zhang, R.; Wang, L.; Deng, R.; Luo, Y. Inhibition on Chloroaromatics during Thermal Conversion Processes of Municipal Solid Waste by Oxygen-Induced Low-Temperature Pre-Dechlorination and Hydrogen-Assisted in-Situ Cl Capture. *Fuel Process. Technol.* **2022**, *237*, 107445. https://doi.org/10.1016/j.fuproc.2022.107445.

(53) Soler, A.; Conesa, J. A.; Ortuño, N. Application of Subcritical Water to Dechlorinate Polyvinyl Chloride Electric Wires. *Energies.* **2018**, *11* (10). https://doi.org/10.3390/en11102612.

(54) Lou, F.; Wang, J.; Sun, C.; Song, J.; Wang, W.; Pan, Y.; Huang, Q.; Yan, J. Influence of Interaction on Accuracy of Quantification of Mixed Microplastics Using Py-GC/MS. *J. Environ. Chem. Eng.* **2022**, *10* (3), 108012. https://doi.org/10.1016/j.jece.2022.108012.

(55) Cho, M.-H.; Song, Y.-J.; Rhu, C.-J.; Go, B.-R. Pyrolysis Process of Mixed Microplastics Using TG-FTIR and TED-GC-MS. *Polymers.* **2023**, *15* (1), 241. https://doi.org/10.3390/polym15010241.

(56) Coralli, I.; Giorgi, V.; Vassura, I.; Rombolà, A. G.; Fabbri, D. Secondary Reactions in the Analysis of Microplastics by Analytical Pyrolysis. *J. Anal. Appl. Pyrolysis.*

**2022**, *161*, 105377. https://doi.org/10.1016/j.jaap.2021.105377.

(57) Fabbri, D.; Tartari, D.; Trombini, C. Analysis of Poly(Vinyl Chloride) and Other Polymers in Sediments and Suspended Matter of a Coastal Lagoon by Pyrolysis-Gas Chromatography-Mass Spectrometry. *Anal. Chim. Acta.* **2000**, *413* (1), 3–11. https://doi.org/10.1016/S0003-2670(00)00766-2.

(58) Sun, Y.; Tang, J.; Mo, Y.; Geng, X.; Zhong, G.; Yi, X.; Yan, C.; Li, J.; Zhang, G. Polycyclic Aromatic Carbon: A Key Fraction Determining the Light Absorption Properties of Methanol-Soluble Brown Carbon of Open Biomass Burning Aerosols. *Environ. Sci. Technol.* **2021**, *55* (23), 15724–15733. https://doi.org/10.1021/acs.est.1c06460.

(59) Yi, X.; Geng, X.; Mo, Y.; Zhong, G.; Tang, J.; Zhu, S.; Cheng, Z.; Zhao, S.; Li, J.; Gustafsson, Ö.; Peng, P.; Zhang, G. Compound-Specific Radiocarbon Analysis of Benzene Polycarboxylic Acids for Source Apportionment of Polyaromatic Organic Matter in Ambient Aerosols. *Atmos. Environ.* **2023**, *307*, 119832. https://doi.org/10.1016/j.atmosenv.2023.119832.

(60) Hassan, S. S.; Williams, G. A.; Jaiswal, A. K. Emerging Technologies for the Pretreatment of Lignocellulosic Biomass. *Bioresour. Technol.* **2018**, *262*, 310–318. https://doi.org/10.1016/j.biortech.2018.04.099.

(61) Chio, C.; Sain, M.; Qin, W. Lignin Utilization: A Review of Lignin Depolymerization from Various Aspects. *Renew. Sustain. Energy Rev.* **2019**, *107*, 232–249. https://doi.org/10.1016/j.rser.2019.03.008.

(62) Zhu, X.; Huang, W.; Fang, M.; Liao, Z.; Wang, Y.; Xu, L.; Mu, Q.; Shi, C.; Lu, C.; Deng, H.; Dahlgren, R.; Shang, X. Airborne Microplastic Concentrations in Five Megacities of Northern and Southeast China. *Environ. Sci. Technol.* **2021**, *55* (19), 12871–12881. https://doi.org/10.1021/acs.est.1c03618.

(63) Xu, Y.; Ou, Q.; Jiao, M.; Liu, G.; van der Hoek, J. P. Identification and Quantification of Nanoplastics in Surface Water and Groundwater by Pyrolysis Gas Chromatography–Mass Spectrometry. *Environ. Sci. Technol.* **2022**, *56* (8), 4988–4997. https://doi.org/10.1021/acs.est.1c07377.

(64) Li, P.; Lai, Y.; Zheng, R.; Li, Q.; Sheng, X.; Yu, S.; Hao, Z.; Cai, Y.; Liu, J. Extraction of Common Small Microplastics and Nanoplastics Embedded in Environmental Solid Matrices by Tetramethylammonium Hydroxide Digestion and Dichloromethane Dissolution for Py-GC-MS Determination. *Environ. Sci. Technol.* **2023**, *57* (32), 12010–12018. https://doi.org/10.1021/acs.est.3c03255.

(65) Zhou, Z.; Ouyang, D.; Liu, D.; Zhao, X. Oxidative Pretreatment of Lignocellulosic Biomass for Enzymatic Hydrolysis: Progress and Challenges. *Bioresour. Technol.*

**2023**, *367*, 128208. https://doi.org/10.1016/j.biortech.2022.128208.

(66) Silverstein, R. A.; Chen, Y.; Sharma-Shivappa, R. R.; Boyette, M. D.; Osborne, J. A Comparison of Chemical Pretreatment Methods for Improving Saccharification of Cotton Stalks. *Bioresour. Technol.* **2007**, *98* (16), 3000–3011. https://doi.org/10.1016/j.biortech.2006.10.022.

(67) Wang, Q.; Wang, Z.; Shen, F.; Hu, J.; Sun, F.; Lin, L.; Yang, G.; Zhang, Y.; Deng, S. Pretreating Lignocellulosic Biomass by the Concentrated Phosphoric Acid plus Hydrogen Peroxide (PHP) for Enzymatic Hydrolysis: Evaluating the Pretreatment Flexibility on Feedstocks and Particle Sizes. *Bioresour. Technol.* **2014**, *166*, 420–428. https://doi.org/10.1016/j.biortech.2014.05.088.

(68) Dong, D.; Sun, J.; Huang, F.; Gao, Q.; Wang, Y.; Li, R. Using Trifluoroacetic Acid to Pretreat Lignocellulosic Biomass. *Biomass Bioenergy.* **2009**, *33* (12), 1719–1723. https://doi.org/10.1016/j.biombioe.2009.07.013.

(69) Naidoo, T.; Goordiyal, K.; Glassom, D. Are Nitric Acid (HNO3) Digestions Efficient in Isolating Microplastics from Juvenile Fish? *Water. Air. Soil Pollut.* **2017**, *228* (12), 470. https://doi.org/10.1007/s11270-017-3654-4.

(70) Catarino, A. I.; Thompson, R.; Sanderson, W.; Henry, T. B. Development and Optimization of a Standard Method for Extraction of Microplastics in Mussels by Enzyme Digestion of Soft Tissues. *Environ. Toxicol. Chem.* **2017**, *36* (4), 947–951. https://doi.org/10.1002/etc.3608.

(71) Liu, K.; Wang, X.; Fang, T.; Xu, P.; Zhu, L.; Li, D. Source and Potential Risk Assessment of Suspended Atmospheric Microplastics in Shanghai. *Sci. Total Environ.* **2019**, *675*, 462–471. https://doi.org/10.1016/j.scitotenv.2019.04.110.

(72) Yuan, Z.; Pei, C.-L.; Li, H.-X.; Lin, L.; Hou, R.; Liu, S.; Zhang, K.; Cai, M.-G.; Xu, X.-R. Vertical Distribution and Transport of Microplastics in the Urban Atmosphere: New Insights from Field Observations. *Sci. Total Environ.* **2023**, *895*, 165190. https://doi.org/10.1016/j.scitotenv.2023.165190.

(73) Wiesinger, H.; Wang, Z.; Hellweg, S. Deep Dive into Plastic Monomers, Additives, and Processing Aids. *Environ. Sci. Technol.* **2021**, *55* (13), 9339–9351. https://doi.org/10.1021/acs.est.1c00976.

(74) Sun, A.; Wang, W.-X. Human Exposure to Microplastics and Its Associated Health Risks. *Environ. Health.* **2023**, *1* (3), 139–149. https://doi.org/10.1021/envhealth.3c00053.

(75) Wang, C.; Wu, W.; Pang, Z.; Liu, J.; Qiu, J.; Luan, T.; Deng, J.; Fang, Z. Polystyrene Microplastics Significantly Facilitate Influenza A Virus Infection of

Host Cells. *J. Hazard. Mater.* **2023**, *446*, 130617. https://doi.org/10.1016/j.jhazmat.2022.130617.

(76) Hu, L.; Feng, X.; Lan, Y.; Zhang, J.; Nie, P.; Xu, H. Co-Exposure with Cadmium Elevates the Toxicity of Microplastics: Trojan Horse Effect from the Perspective of Intestinal Barrier. *J. Hazard. Mater.* **2024**, *466*, 133587. https://doi.org/10.1016/j.jhazmat.2024.133587.

(77) da Costa Araújo, A. P.; Malafaia, G. Microplastic Ingestion Induces Behavioral Disorders in Mice: A Preliminary Study on the Trophic Transfer Effects via Tadpoles and Fish. *J. Hazard. Mater.* **2021**, *401*, 123263. https://doi.org/10.1016/j.jhazmat.2020.123263.

(78) Eberhard, T.; Casillas, G.; Zarus, G. M.; Barr, D. B. Systematic Review of Microplastics and Nanoplastics in Indoor and Outdoor Air: Identifying a Framework and Data Needs for Quantifying Human Inhalation Exposures. *J. Expo. Sci. Environ. Epidemiol.* **2024**, 1–12. https://doi.org/10.1038/s41370-023-00634-x.

(79) Prata, J. C.; Padrão, J.; Khan, M. T.; Walker, T. R. Do's and Don'ts of Microplastic Research: A Comprehensive Guide. *Water Emerg. Contam. Nanoplastics.* **2024**, *3* (2), 8. https://doi.org/10.20517/wecn.2023.61.

(80) International Organization for Standardization. Principles for the Analysis of Microplastics Present in the Environment; ISO 24187:2023(E); Vernier, Geneva, 2023.